# Electrophoretic Behavior of Amphiphilic Diblock Copolymer Micelles

**Aurélie Morel,[†] Hervé Cottet,*[,‡] Martin In,[†] Sophie Deroo,[§] and Mathias Destarac[§]**

*Laboratoire des Colloïdes, Verres et Nanomatériaux, UMR CNRS 5587, Université Montpellier 2, place Eugène Bataillon CC 026, 34095 Montpellier Cedex 5, France; Laboratoire Organisation Moléculaire, Evolution et Matériaux Fluorés, UMR 5073, Université Montpellier 2, place Eugène Bataillon CC 017, 34095 Montpellier Cedex 5, France; and Rhodia, Centre de Recherches et Technologies, 52 rue de la Haie Coq 93308 Aubervilliers, Cedex, France*

*Received March 21, 2005; Revised Manuscript Received May 25, 2005*

ABSTRACT: Aqueous solutions of poly(vinyl acetate)-*b*-sodium polyacrylate (PVAc-*b*-NaPAA) block copolymers were characterized by capillary electrophoresis (CE). CE experiments reveal the presence of NaPAA dead chains, acetate ions (which are a byproduct of the hydrolysis of PVAc), and nonassociated copolymers (unimers). This fraction of unimers is dependent on the chemical composition of the copolymers and on the purification procedure. It remains constant when increasing copolymer concentration. The fraction of unimers was too high to correspond to a critical micellar concentration. Instead, this high content of unimers is likely due to the polydispersity in composition of the copolymers, sodium polyacrylate-rich copolymers being excluded from the micellization process. This interpretation is consistent with the study of the effect of temperature on the free copolymer fraction. Above a temperature threshold, the unimer population increases due to the destabilization of part of the micelles. Addition of a neutral surfactant leads to the formation of mixed micelles, the electrophoretic mobility of which can be modeled using recent theoretical developments on electrokinetic migration of composite objects.

## 1. Introduction

Recent advances in copolymer chemistry extended the realm of associative copolymers. Classical questions raised in the study of self-assembling systems regard the critical micelle concentration, the equilibrium structure of the self-assemblies obtained, and the kinetics of exchange. It has been shown that the same types of structures are obtained with amphiphilic copolymers as with surfactant, following the same rules of packing-determined curvature.[1] However, the critical micelle concentration (cmc) of amphiphilic copolymers can be several orders of magnitude lower than that of surfactants. Moreover, the kinetics of exchange between the free and micellized states can be very slow or even frozen for copolymer systems, while it is generally fast (on the order of microseconds) for surfactant micelles. Also, the size of the macromolecule prevents crystallization as a purification procedure and leads necessarily to some polydispersity in size and composition. Although good control can be achieved today, copolymers that are the most likely to have industrial impact present in general polydispersity indexes large enough to have a great influence on the association behavior. Our contribution aims at showing that both aspects of synthesis control and association behavior of amphiphilic polyelectrolytes can be addressed by capillary electrophoresis.

To characterize copolymer micelle systems, many experimental techniques are required. For details on the different techniques, and on the information that can be derived from them, see ref 2. These methods include static and dynamic light scattering which can bring information on micelle dimensions (respectively on the radius of gyration, $R_g$, and on the hydrodynamic radius, $R_h$). Neutron scattering gives finer details of the structure of the micelles.[3] Sedimentation and viscosity experiments may also provide useful information on molecular masses, when combined with dynamic light scattering experiments.[2] Separation techniques such as size-exclusion chromatography (SEC) or capillary electrophoresis (CE) are also very informative to (i) quantify the fraction of unimers in the micellar solution, (ii) characterize the size and/or the polydispersity of the micelles, (iii) study the kinetics of exchange between unimers and micelles, and (iv) investigate possible interactions between micelles, unimers, and other solutes.

In previous works a significant population of unassociated unimers was separated from the micelles by either SEC[4] or CE.[5] This population of free copolymers (unimers) was quantified at a concentration much higher than the cmc for different copolymer systems such as polystyrene−poly(ethylene oxide) (PS-*b*-PEO),[4] poly(ethylene−propylene)-*b*-poly(styrenesulfonate) (PEP−PSS),[5] poly(*tert*-butylstyrene)-*b*-poly(styrenesulfonate) (PtBS-*b*-PSS),[5] and poly(butyl acrylate)-*b*-poly(acrylic acid) (PABu-*b*-PAA).[6] Xu et al.[4] have demonstrated on PS−PEO copolymers in water using the off-line coupling of SEC with infrared spectroscopy that this population of unimers corresponds to a lower hydrophobic/hydrophilic monomer ratio than the average one. The concentration of unassociated unimer was found to increase with overall concentration of copolymer even above the cmc.[5,7]

In practice, the determination of micelle dimensions and polydispersity by SEC is difficult due to (i) interactions between copolymers and the stationary phase and (ii) the lack of suitable calibration. The first difficulty is often addressed by addition of organic solvent in the mobile phase, which modifies also the micellization process.[6] Although not widely used in the field of synthetic polymer analysis, CE has the advantage over

[†] UMR CNRS 5587, Université Montpellier 2.
[‡] UMR 5073, Université Montpellier 2.
[§] Centre de Recherches d'Aubervilliers Rhodia 52.
* Corresponding author: Tel +33 4 6714 3427; Fax +33 4 6763 1046; e-mail hcottet@univ-montp2.fr.

10.1021/ma050586f CCC: $30.25 
Published on Web 06/28/2005

SEC that there is no stationary phase. Moreover, the interaction with the capillary wall can be minimized either by a judicious adjustment of the pH of the electrolyte or by using coated capillaries. Because of the opportunity to use mild conditions (relatively low ionic strength, pure aqueous medium, absence of stationary phase) that are relatively close to the conditions of applications, CE is a promising method to study copolymer micelle systems.

Morishima used CE to monitor the collapse of self-assembling amphiphilic polyelectrolytes upon increasing the content of hydrophobic monomers in the copolymer.[8] Using EC, Cottet et al.[5] pointed out the presence of unimers of PEP-*b*-PSS or PtBS-*b*-PSS and noticed that they interacted with neutral surfactant micelles, while the micellized copolymer did not. In the same work, the influence of the electric field, the temperature, and the addition of organic solvent on the electrophoretic behavior of the associative copolymer system were investigated. Stepanek et al.[9] used CE as a tool to prove the formation of mixed copolymer micelles, obtained by dialysis in a dioxane/water mixture against water, from two diblock copolymers: PS-*b*-poly(methacrylic acid) and PS-*b*-PEO.

Recently, a new process of controlled radical polymerization coined macromolecular design via the interchange of xanthates (MADIX) and based on the use of dithiocarbonates (xanthates) as reversible chain transfer agents was developed.[10,11] It allows direct synthesis of amphiphilic poly(vinyl acetate)-*b*-poly(acrylic acid), PVAc-*b*-PAA, block copolymers in solution. From the main techniques of controlled free radical polymerization, MADIX was the first straightforward technique to be applicable for the controlled polymerization of VAc.[10,11]

The purpose of this work was to study the electrophoretic behavior of PVAc-*b*-NaPAA charged block copolymer micelles and to point out the potential of CE to characterize new diblock copolymer systems.

## 2. Electrophoretic Mobility

**2.1. Principle of Capillary Electrophoresis.** Capillary electrophoresis is an analytical separation technique based on the differential migration of ionic species under electric field.[12] It employs narrow-bore (25−200 $\mu$m) capillaries to perform high-efficiency separations using very high electric field (typically higher than 500 V/cm). In capillary zone electrophoresis (CZE), the capillary is filled with buffer, and both ends of the capillary are placed in reservoirs containing the same buffer. In CZE the buffer composition and the electric field are constant all along the length of the capillary. The apparent electrophoretic mobility $\mu_{app}$ of the solute is defined according to eq 1:

$$\mu_{app} = \frac{v_{app}}{E} = \frac{Ll}{Vt_{app}} \quad (1)$$

where $v_{app}$ is the apparent electrophoretic velocity, $E$ ($V/L$) is the electric field, $L$ is the total capillary length, $l$ is the migration distance, $V$ is the applied voltage, and $t_{app}$ is the apparent migration time of the solute. The apparent mobility is the sum of two distinctive contributions: one pertaining to the own electrophoretic motion of the solute (effective electrophoretic mobility, $\mu_{ep}$) and the other pertaining to the electroosmotic flow ($\mu_{eo}$). Electroosmosis refers to the movement of an electrolyte solution in a capillary under the influence of an electric field. Under basic conditions (pH > 7), the negatively charged wall of the fused silica capillary attracts positively charged ions of the buffer, creating an electrical double layer. When a voltage is applied across the capillary, cations of the double layer migrate in the direction of the cathode, carrying water molecules with them and generating the so-called electroosmotic flow. Thus, the effective electrophoretic mobility is related to the apparent electroosmotic ($\mu_{eo}$) mobilities according to eq 2:

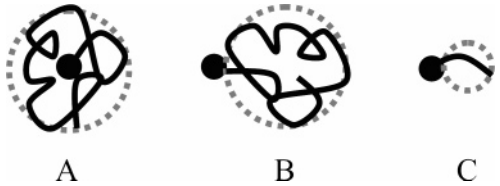


**Figure 1.** Schematic representation of possible conformations of composite object composed of a hydrodynamic ball and a polyelectrolyte chain. (A) The hydrodynamic ball is fully wrapped by a polyelectrolyte chain. (B, C) There is a segregation between the ball and the polyelectrolyte chain, the latter being either in coil (B) or a rigid (C) conformation.

$$\mu_{ep} = \mu_{app} - \mu_{eo} = \frac{Ll}{Vt_{app}} - \frac{Ll}{Vt_{eo}} \quad (2)$$

where $t_{eo}$ is the migration time of a neutral molecule. It is worth noting that mobilities are algebraic values. Cations have positive $\mu_{ep}$ values while anions have negative $\mu_{ep}$ values.

**2.2. Theoretical Background: Mobility of Composite Objects Constituted of a Polyelectrolyte Tail and a Neutral Ball.** This section focuses on the modelization of the electrophoretic mobility of composite objects that could help to understand the electrophoretic behavior of block copolymer systems. Electrophoresis of composite object was studied by Anderson et al.[13] and by Long et al.[14,15] Figure 1 depicts different possible conformations for composite objects composed of a polyelectrolyte tail and a neutral ball. In this picture, the neutral ball represents either the hydrophobic block of the unimer or a neutral surfactant micelle that is linked to the hydrophobic block by hydrophobic interaction.

We report equations established by Long et al.[14,15] that allow to model the electrophoretic mobility of composites objects constituted of charged and neutral subunits. The conformation of the composite object, and thus the choice of the relevant model, depends on the dimension of the neutral ball, the contour length, the stiffness of the polyelectrolyte (persistence length), and possibly the electric field.

**2.2.1. Hydrodynamic Coupling between the Neutral Ball and the Polyelectrolyte Tail.** When the neutral ball is fully wrapped by the polyelectrolyte chain (Figure 1A), there is strong hydrodynamic coupling between the ball and the polyelectrolyte chain. In this case, the electrophoretic mobility of the composite object expresses as the number-average of the electrophoretic mobilities calculated on all the hydrodynamically equivalent independent "blobs" constituting the object.[15,16] This model holds only if the dimension of the equivalent blobs is taken higher than or equal to the Debye length. A simple manner to define the equivalent "blob" dimension is to choose the dimension of the neutral ball as a reference (if its dimension is equal to or higher than the Debye length). Dividing the polyelectrolyte chain in

$N$ equivalents blobs, the electrophoretic mobility $\mu_{ep}$ of the composite object is the number-average electrophoretic mobility calculated on the $N + 1$ blobs:[16]

$$\mu_{ep} = \frac{\sum_{i=1}^{N+1} \mu_{ep}^{i}}{N+1} = \frac{\mu_{ep}^{0}}{1 + \frac{\alpha}{DP_0}} \tag{3}$$

where $\mu_{ep}^{0}$ is the free-draining mobility of the polyelectrolyte chain (independent of the chain length), $DP_0$ is the degree of polymerization of the polyelectrolyte chain in composite object, and α is the number of charged monomers contained in one equivalent blob. α depends on the dimension of the neutral ball and on the persistence length of the polyelectrolyte chain.

**2.2.2. No Hydrodynamic Coupling between the Neutral Ball and the Polyelectrolyte Chain. 2.2.2.1. Polyelectrolyte Chain in Coil Conformation.** The conformation depicted in Figure 1B corresponds to segregation between the neutral ball and the polyelectrolyte chain. In this case, assuming that there is no hydrodynamic coupling between the two composite moieties and that the polyelectrolyte chain does not stretch during the electrophoretic process, the electrophoretic mobility of the composite object is given by the average electrophoretic mobility of the two moieties weighted by their hydrodynamic friction coefficient $\gamma$. Using the Stokes equation for the hydrodynamic frictional coefficient of a spherical object, the electrophoretic mobility $\mu_{ep}$ is thus obtained by[14,16]

$$\mu_{ep} = \frac{\sum_{i=0}^{1} \gamma_i \mu_{ep}^{i}}{\sum_{i=0}^{1} \gamma_i} = \frac{\mu_{ep}^{0}}{1 + \frac{R_B}{R_0}} \tag{4}$$

where $\gamma_i$ is the hydrodynamic frictional coefficient of the moiety $i$, $R_0$ is the hydrodynamic radius of the polyelectrolyte chain, and $R_B$ is the hydrodynamic radius of the neutral ball.

**2.2.2.2. Polyelectrolyte Chain in Fully Stretched Conformation.** For polyelectrolyte chain of relatively short contour lengths and/or for rigid polyelectrolyte chain, the polyelectrolyte conformation can be fully extended (see Figure 1C). Stokes' law is no more appropriated for the frictional coefficient of the polyelectrolyte chain, and the mobility is given by[16]

$$\mu_{ep} = \frac{\sum_{i=0}^{1} \gamma_i \mu_{ep}^{i}}{\sum_{i=0}^{1} \gamma_i} = \frac{\mu_{ep}^{0}}{1 + \frac{2R_B}{a DP_0} \ln DP_0} \tag{5}$$

where $a$ is the dimension of a charged monomer in the polyelectrolyte chain. This equation is obtained by replacing in (4) the expression of the hydrodynamic frictional coefficient of a rigid rod in random orientation with respect to the flow direction:

$$\gamma_{rod} = \frac{3\pi\eta a DP_0}{\ln(DP_0)} \tag{6}$$

where $\eta$ is the solvent viscosity.

**2.2.3. Characteristic Dimensions.** To identify the relevant model corresponding to the copolymer composition and the electrolyte, some characteristic dimensions have to be estimated. First, the Debye length is 1.1 nm for an ionic strength of 80 mM (160 mM borate buffer, pH 9.2). The persistence length of the polyelectrolyte chain (sodium polyacrylate, NaPAA) is $l_p = 5.1$ nm, so about 16 monomers at 100 mM ionic strength (NaBr at 25 °C).[17] The hydrodynamic radius of the PAA chain, $R_{PAA}$, and that of the PVAc block, $R_{PVAc}$, depend on the degree of polymerization of each block. $R_{PAA}$ (in nm) was calculated using eq 7. It is derived from the Mark−Houwink−Sakurada equation using the parameters of sodium polyacrylate at an ionic strength $I = 0.1$ M (NaBr) and a temperature $T = 25$ °C.[17]

$$R_{PAA} = \left(\frac{3[\eta]M_{PAA}}{10\pi N_A}\right)^{1/3} = 0.09654 DP_{PAA}^{0.585} \tag{7}$$

with $M_{PAA}$ the molecular weight of the PAA block (in g/mol).

$R_{PVAc}$ was estimated by the incompressibility condition of a polymer in melt:

$$R_{PVAc} = \left(\frac{3}{4\pi} \frac{DP_{PVAc} M_{VAc}}{\rho_{PVAc} N_A}\right)^{1/3} \tag{8}$$

$R_{PVAc}$ and $R_{PAA}$ are reported in Table 2 for different copolymer samples. For all copolymer samples, the radius of gyration of PVAc blocks was slightly higher than the Debye length (see Table 2). Thus, in the model described in section 2.2.1 and for a composite object corresponding to one unimer, the dimension of one equivalent blob can be taken as $2R_{PVAc}$. Moreover, the dimension of the neutral ball ($2R_{PVAC}$) is always smaller than $l_p$. Consequently, α, the number of charged monomers in one equivalent blob, equals to $2R_{PVAC}/a$.

The hydrodynamic radius of a micelle of Brij 35 (polyoxyethylene 23 dodecyl ether) was found to be about 4.3 nm in similar conditions (50 °C in a 40 mM borate buffer).[18]

**Table 1. Physicochemical Characteristics of the Copolymer Micelles in Brine Solution (NaCl) at pH 9 and Ionic Strength $I = 0.5$ M[a]**

| copolymer designation | $R_g$ (nm) | $R_h$ (nm) | $N$ |
|---|---|---|---|
| 115−140 | 11 | 40 | 60 |
| 75−20 | 11 | 22 | 90 |
| 185−55 | 20 | 50 | 200 |

[a] $R_g$ = radius of gyration, $R_h$ = hydrodynamic radius, and $N$ = aggregation number of the micelles.

## 3. Materials and Methods

**3.1. Reagents.** Borax (disodium tetraborate decahydrate) was purchased from Prolabo (Paris, France). Mesityl oxide, the neutral surfactant polyoxyethylene 23 dodecyl ether (Brij 35), and *N*-tris(hydroxymethyl)methyl-3-aminopropanesulfonate (TAPS) were obtained from Aldrich (Milwaukee, WI). The water used to prepare all buffers was delivered by an Alpha-Q system (Millipore, Molsheim, France). The 160 mM borate

**Table 2. Hydrodynamic Radii of PVAc and PAA Blocks, Effective Electrophoretic Mobility Values for the Diblock Copolymer System (Micelle ($\mu_{ep}^1$), Unimer ($\mu_{ep}^2$), Residual PAA ($\mu_{ep}^0$)), and Fraction of Unimers (A)[a]**

| copolymer ($DP_{PVAc}-DP_{PAA}$) | $R_{PAA}$[b] (nm) | $R_{PVAc}$[b] (nm) | electrophoretic mobilities ($10^{-9}$ m$^2$ V$^{-1}$ s$^{-1}$) | | | | $A$[d] |
|---|---|---|---|---|---|---|---|
| | | | $\mu_{ep}^1$ (peak 1) | $\mu_{ep}^2$ (peak 2) | $(\mu_{ep}^2)_{eq\ 3}$[c] | $\mu_{ep}^0$ (peak 3) | |
| $115-140^{(2)}$ | 1.39 | 1.50 | −30.4 | −32.1 | −32.1 | −34.5 | 0.26 |
| $115-140^{(3)}$ | 1.39 | 1.50 | −31.9 | −33.1 | −32.1 | −35.5 | 0.48 |
| $75-20^{(1)}$ | 0.59 | 1.28 | −30.7 | | −24.8 | | |
| $185-55^{(2)}$ | 1.02 | 1.75 | −30.3 | −31.9 | −28.5 | −35.0 | 0.11 |
| $185-55^{(3)}$ | 1.02 | 1.75 | −31.9 | −32.3 | −28.5 | −35.0 | 0.18 |

[a] The confidence interval on electrophoretic mobilities calculated on five experiments (confidence level 0.95) is $0.3 \times 10^{-9}$ m$^2$ V$^{-1}$ s$^{-1}$. [b] Radii of each copolymer block were calculated using eqs 7 and 8. [c] The electrophoretic mobility of the unimer was calculated according to eq 3 taking the average chemical composition from synthesis conditions. α value in eq 3 was calculated according to section 2.2.3. [d] The fraction of free unimers in the samples was calculated from the ratio of the time-corrected area of peak 2 to the sum of the time-corrected areas of peaks 1 and 2.

buffer, pH 9.2, was directly prepared by dissolving the appropriate amount of Borax in water.

**3.2. Diblock Copolymers.** Three diblock copolymers of vinyl acetate and sodium acrylate were studied in this work: 75−20, 115−140, and 185−55, where the copolymers are referred to as ($DP_{PVAc}-DP_{PAA}$), DP being the degree of polymerization of each block. The diblock copolymers were synthesized by controlled radical polymerization in solution in two steps. The first step leads to xanthate-functionalized poly(acrylic acid), which is used in the second step as precursor for the synthesis of the poly(vinyl acetate) block. The xanthate function of the final copolymer terminates the PVAc block. Both polymerization steps proceed in an organic solvent or a water/solvent mixture.

Purification of the diblocks proceeds according to three different methods, depending on the asymmetry parameter. 75−20 was purified in its acidic form by precipitation in deionized water (method 1). The other ones, 115−140 and 185−55, were precipitated as sodium salt in a water/acetone mixture (75/25 w/w) (method 2) or by dialysis against deionized water for 1 week (method 3). The membrane used is Cellu Sep T4 (of width 45 mm and thickness 20 μm) with a molecular weight cutoff of 12 000−14 000 Da.

One of the copolymer (115−140) was characterized by size-exclusion chromatography experiments (SEC) coupled with multiangle laser light scattering (MALLS) experiments after full hydrolysis of the PVAc block. The polydispersity index was 1.8, and the number-average molecular weight (PEO calibration) was 22 000 g/mol.

The acid acrylic content of all copolymers measured by potentiometric titration was close to the expected value. Homopolymer of PAA was sometime detected by SEC or CE and was hardly eliminated by the dialysis process as performed. Proton NMR performed on the acidic form of the purified copolymers dissolved in a $d_6$-DMSO showed that the hydrolysis rate of the PVAc block was less than 7% molar.

50 g/L stock sample solutions of copolymers were prepared by dissolving the solid product in water for the diblocks purified as sodium salt and in aqueous sodium hydroxide solutions for diblocks purified in acidic form. Care was taken to get the right amount of sodium hydroxide. Unless otherwise specified, solutions were further diluted five times with the separation electrolyte used for EC.

As evidenced by small-angle neutron scattering and dynamic light scattering measurements,[19] the diblock copolymers studied in this work form micelles in aqueous solutions. Characteristic dimensions of the copolymer micelles in brine at pH = 9 and for an ionic strength of 0.5 M are given in Table 1. The hydrodynamic radius $R_h$ is measured by dynamic light scattering, the radius of gyration $R_g$ is obtained from small-angle neutron scattering experiments, and the aggregation number is estimated from the molecular weight of the micelles divided by the theoretical molecular weight of the copolymer.[19]

**3.3. Capillary Electrophoresis.** The CE experiments were performed using an Agilent Technologies $^{3D}$CE capillary electrophoresis system. Separation capillaries were prepared from bare silica tubing purchased from Composite Metal Services (Worcester, United Kingdom). Capillary dimensions were 33.5 cm (25 cm to the detector) × 50 μm i.d. New capillaries were conditioned with the following flushes: 1 M NaOH for 30 min, 0.1 M NaOH for 30 min, and water for 10 min. Samples were introduced hydrodynamically (∼4 nL) by application of a positive pressure on the inlet side of the capillaries (17 mbar for 3 s). Mesityl oxide (∼0.1% (v/v) in the borate buffer) was injected as a neutral marker to determine the electroosmotic mobility. The applied potential was +8 kV. Copolymers were monitored spectrophotometrically by UV absorbance at two different wavelengths: 200 and 290 nm, the latter being xanthate specific. The temperature of the capillary cartridge was set at 30 °C, unless otherwise specified.

For a better comparison between the copolymer samples and to correct the electrophoretic mobilities from the electroosmotic flow (EOF) fluctuations, the electropherograms are plotted using an effective (EOF-corrected) electrophoretic mobility scale. The current electropherograms (absorbance vs $t_{app}$) were translated in effective mobility scale (absorbance vs $\mu_{ep}$) using eq 2. The confidence interval (confidence level 0.95) on effective mobility values determined on five successive runs is $\pm 0.3 \times 10^{-9}$ m$^2$ V$^{-1}$ s$^{-1}$.

In CZE, concentrations of the solutes are proportional to peak areas divided by $t_{app}$ (so-called time-corrected areas).[12]

## 4. Results and Discussion

**4.1. Typical Electropherograms and Peak Assignments.** The electropherograms of the copolymers, purified according to one of the three methods described in section 3.2, are presented in Figure 2.

The first electropherogram (Figure 2A) corresponds to the 75−20 copolymer. It is characterized by a main peak (noted 1 in Figure 2A) with an effective electrophoretic mobility $\mu_{ep} = -30.7 \times 10^{-9}$ m$^2$ V$^{-1}$ s$^{-1}$ and a much smaller one (noted i) at $-29.4 \times 10^{-9}$ m$^2$ V$^{-1}$ s$^{-1}$. The second electropherogram (Figure 2B) also concerns a PVAc dominant copolymer (185−55). It presents two peaks: a main one at $-30.3 \times 10^{-9}$ m$^2$ V$^{-1}$ s$^{-1}$ (noted 1) and a second one corresponding to more mobile species at $-31.9 \times 10^{-9}$ m$^2$ V$^{-1}$ s$^{-1}$ (noted 2). Peaks 1 and 2 have been respectively assigned to copolymer micelles and to unimers. This will be justified in detail in section 4.1.3. Peak i has not yet been assigned, but it does not correspond to copolymer chains since it was not detected at 290 nm.

The third electropherogram concerns the 115−140 copolymer and shows as many as four peaks. Two of them have the same electrophoretic mobility as peaks 1 and 2 in electropherogram B. Both extra peaks are located at $-34.4 \times 10^{-9}$ m$^2$ V$^{-1}$ s$^{-1}$ (peak 3) and $-36.6 \times 10^{-9}$ m$^2$ V$^{-1}$ s$^{-1}$ (peak 4). They are respectively characteristic of a free-draining NaPAA (electrophoretic mobility independent of the polymerization degree) and acetate ions. Peak 3 and 4 have been assigned by spiking the sample with PAA of $10^4$ g/mol molecular

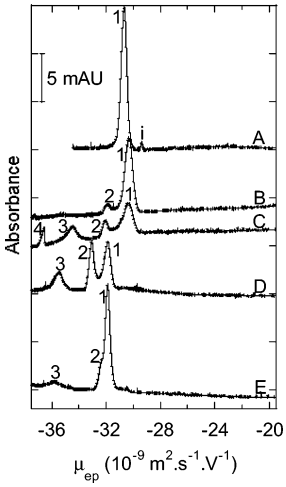


**Figure 2.** Electropherograms of the diblock copolymers 75−20 (A) purified according to method 1; 185−55 purified according to method 2 (B), 115−140 purified according to methods 2 (C), 115−140 purified according to methods 3 (D), and 185−55 purified according to methods 3 (E). Fused silica capillary, 33.5 cm (25 cm to the detector) × 50 $\mu$m i.d. Electrolyte: 180 mM borate buffer, pH 9.2. Applied voltage: +8 kV. Hydrodynamic injection: 17 mbar, 3 s. UV detection at 200 nm. Temperature: 30 °C. Identifications: peak 1, copolymer micelles; peak 2, nonassociated block copolymers; peak 3, PAA dead chains; peak 4, acetate; peak i, unidentified impurity.

mass and sodium acetate (not shown). Electropherograms D and E in Figure 2 show that the number of detected peaks as well as their intensity depend also on the purification procedure. This will be further discussed in sections 4.2.1 and 4.2.2.

**4.1.1. Residual Homopolymer.** Owing to the polymerization mechanism, PAA chains can be generated without the xanthate group or can lose it. This leads to so-called dead chains that cannot copolymerize further with vinyl acetate monomers. The absence of xanthate on the dead PAA homopolymer was confirmed by the absence of peak 3 when detection proceeds at 290 nm. Since the PAA homopolymer does not bear any neutral block, its electrophoretic mobility was higher (in absolute value) than that of the unimer (peak 2). By separating PAA from copolymer unimer and copolymer micelles, CE can bring interesting information to the polymer chemist about the proportion of dead polymer chain at the final stage of the synthesis. However, the presence of PAA in the copolymer sample depends also on the purification procedure: if the nonhydrolyzed diblocks were purified by precipitation in water, peak 3 was not detected (see Figure 2A). The residual PAA, which is soluble in water, was eliminated in the supernatant. On the other hand, dialysis did not remove residual PAA from the copolymer solution as pointed out by the comparison between electropherograms B and E in Figure 2. Note that the precipitation in a water/acetone mixture (method 2) does not also suppress the PAA chains from the sample (see Figure 2C).

**4.1.2 Acetate Ion and Postpolymerization Hydrolysis of the Copolymer.** Acetate ion is a degradation product from the hydrolysis of the PVAc block in basic medium. Hydrolysis of the diblock copolymer during its storage can be evidenced by CE as demonstrated in Figure 2C by the detection of acetate ions (peak 4). The presence of acetate in the sample depends also on the purification procedure: acetate was not present on the electropherogram corresponding to the 115−140 dialyzed diblock (see Figure 2D), while it was detected for the same diblock when purified by precipitation (Figure 2C).

**4.1.3. Assignment of Peaks 1 and 2.** Peaks 1 and 2 were assigned to copolymer molecules because these peaks were also detected at 290 nm, a characteristic wavelength of the terminal xanthate group (not shown). In self-assembling systems, two populations are expected: micelles and free unimers. In principle, the concentration of free unimers cannot exceed the critical micelle concentration (cmc). Moreover, the cmc of such diblock copolymers is expected to be rather low and certainly lower than the detection limit of the UV detector. Thus, only the copolymer micelles should be detected in CE experiments using UV detection. The electropherogram of the 75−20 copolymer (Figure 2A) is representative of what would be expected. It displays only one peak corresponding to copolymer micelles. The other electropherograms in Figure 2 exhibit two copolymer peaks (peaks 1 and 2).

Micelles are expected to be predominant in amphiphilic copolymer solutions. It is thus reasonable to assign the major peak (peak 1) to micelles and the other (peak 2) to unimers. As already discussed in the Introduction, significant amounts of unimer in diblock copolymer systems have actually been observed previously.[4,5] This high concentration in unimers was explained by the polydispersity of the copolymer. As demonstrated by Xu et al.,[4] these unimers are enriched in hydrophilic monomers in comparison with the copolymer constituting the micelles. It is worth noting that these unimers do contain hydrophobic monomers since they interact with neutral surfactant micelle (section 4.3.1 and ref 5). However, the hydrophobic/hydrophilic ratio of these unimers is too low to lead to micellization. As expected, the electrophoretic mobility of the unimers (peak 2) is lower (in absolute value) than that of PAA homopolymer (see Table 2) due to the slowing effect of the neutral ball constituted by the hydrophobic block. However, since the unimers in peak 2 have a different (and unknown) chemical composition from that of the copolymer micelles, the knowledge of the right molecular parameters was missing to accurately model the free copolymer electrophoretic mobility using eq 3. Taking the chemical composition of the unimer population as the average composition obtained from the synthesis conditions, the electrophoretic mobility of the unimers $(\mu_{ep}^2)_{eq\ 3}$ was calculated according to eq 3. The values are given in Table 2 and compared to the experimental effective electrophoretic mobility of peak 2, $\mu_{ep}^2$. Since the unimers have higher hydrophilic/hydrophobic monomer ratios, the experimental values are higher (in absolute value) than the theoretical ones. As for previously reported results,[5] the electrophoretic mobility of the copolymer micelles (peak 1) was found to be lower (in absolute value) than that of the free copolymer.

**4.2. Fraction of Unimers.** The fraction of free unimers in the samples was calculated from the ratio of the time-corrected area of peak 2 to the sum of the time-corrected areas of peaks 1 and 2 (see last column of Table 2).

**4.2.1. Influence of the Mode of Purification.** The fraction of free unimers was influenced by the purification method (see Table 2). Whatever the chemical composition of the diblock copolymer, the fraction of unimers was lower when the diblock was purified by

method 2 (precipitation in water/acetone mixture) in comparison with method 3 (dialysis against water).

Another distinction between precipitated and dialyzed copolymer samples is based on the difference in effective mobilities between peaks 1 and 2 (see Table 2). It decreases from $1.7 \times 10^{-9}$ $m^2$ $V^{-1}$ $s^{-1}$ (electropherogram 2C) to $1.2 \times 10^{-9}$ $m^2$ $V^{-1}$ $s^{-1}$ (electropherogram 2D). This reduction in $\mu_{ep}$ is so marked for the 185−55 copolymer that peak 2 appears as a shoulder in peak 1 (electropherogram 2E). These results could be explained by a fractionation during purification process. Precipitation of the sample would lead to enrichment in hydrophobic monomers. Another possibility is to invoke a modification of the path leading to micelles. The self-association process follows different paths depending on the way the selective solvent is introduced, a fact on which relies solvent casting procedures. These results demonstrate the interest of CE to monitor the influence of the diblock preparation mode on the proportion of unassociated unimers.

**4.2.2. Influence of the Copolymer Composition.** The fraction of unimers was higher for a symmetric copolymer such as 115−140 than for a highly hydrophobic copolymer such as 185−55 (see Table 2). For a dissymmetric copolymer with a small hydrophilic block (75−20), it is reasonable to think that a slight difference in chemical composition does not prevent the micellization of the copolymer. In comparison, for a symmetric copolymer, the diblock at the rim of the distribution of composition could become too hydrosoluble to micellize. It is well established that self-assembling results from a balance of opposing forces (repulsion and attraction). For micellization to occur, this balance has to be such that the work of attractive forces compensates for the work of the repulsive forces and for the translational entropy loss. In other words, PAA dominant copolymers (which looks like PAA) are repealed from the corona of the micelles and cannot incorporate their small hydrophobic block into an existing copolymer micelle. However, they can do it with nonionic surfactant micelles (see section 4.3.1).

**4.2.3. Influence of the Diblock Concentration.** The time-corrected peak area relative to the unimers, the micelles, and the PAA increases linearly with the sample concentration. The slopes of these lines were calculated on the 115−140 copolymer (H = 20%) and are respectively 132, 98, and 50 mAU L $g^{-1}$ for peaks 1, 2, and 3. The fraction of peak 2 remained constant with the sample concentration. This situation is very different from classical surfactant micelle where the concentration in unimer remains constant above the cmc, so that the fraction decreases. This observation suggests that the unimers are not involved in the micellization process. Assuming that the copolymer micelles and the unimers have the same extinction coefficient, the 185−55 and 115−140 copolymer systems contain respectively a weight fraction of unimers of 0.11 and 0.26 when precipitated and 0.18 and 0.48 when dialyzed (see Table 2). The 75−20 copolymer does not contain any detectable unimer.

**4.2.4. Influence of the Ionic Strength of the Electrolyte.** The influence of the ionic strength ranging from 10 to 120 mM in borate buffers was studied on the 115−140 copolymer purified by method 2 (precipitation in acetone/water mixture). No influence of the ionic strength on the fraction of unimers was observed, although the aggregation number of the micelle is known to increase with the ionic strength.[19] This result means that when the ionic strength increases, there is a rearrangement between the copolymers coming from the micelles, but the unassociated unimers remain excluded from the self-associating process.

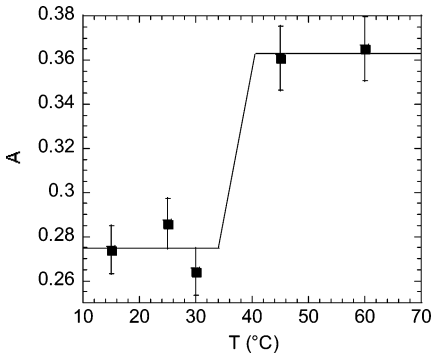


**Figure 3.** Fraction of unimers A vs temperature *T* in 115−140 copolymer aqueous solution at pH 9 and I = 0.5 M. The copolymer was purified according to method 2. Other experimental conditions are the same as in Figure 2.

**4.2.5. Influence of the Temperature.** The influence of the temperature on the free copolymer fraction was next investigated between 15 and 60 °C. Both separation capillary and sample were thermostated. As shown in Figure 3, the fraction of 155−140 unimers in solution was nearly constant at 0.27 up to 30 °C, and then it abruptly increased up to 0.36 with the temperature. When reducing the temperature of the system back to room temperature, the fraction of unimer was reversibly reduced to 0.27. A similar observation but less marked was made on 185−55 solutions: the fraction of unimers increases by 13%, from 0.11 to 0.124, when the temperature was increased above 30 °C. Above 30 °C, a fraction of the copolymer micelles are destabilized and their copolymer chains became unimers. This process led to an increase in the free copolymer population. This abrupt transition at 30 °C is likely related to a softening of the micellar core.[20]

**4.3. Transient Character of the Copolymer Micelles. 4.3.1. Interaction between Diblock Copolymer and Nonionic Surfactant Micelle. 4.3.1.1 Evidence of the Free Copolymer−Surfactant Micelle Interaction.** The electropherograms of two copolymers obtained in the absence and in the presence of a neutral surfactant are compared in Figure 4. It is also shown in this figure (electropherogram C) that PAA homopolymer does not interact with the surfactant micelles.

For the 115−140 and the 185−55 copolymers, peak 2 completely disappears upon addition of Brij 35 (see Figure 4B). An additional broad peak (noted 2*) is observed. Moreover, for the 75−20 copolymer, almost half of the micelle population (peak 1) is also destabilized by the presence of Brij micelles (see Figure 4D). This new peak 2* corresponds to a lower mobility (in absolute value) than that of the copolymer micelle. It is thus attributed to a stable complex buildup from hydrophobic association between a free copolymer and a Brij micelle. The Brij micelle acted as a hydrodynamic ball that reduced the electrophoretic velocity of the unimer. This decrease in the electrophoretic mobility of the unimers after complexation with a Brij micelle was also associated with a broadening of the peak (peaks 2* are much broader than peaks 2). The presence of Brij micelle magnified the influence of the chemical heterogeneity of the copolymer on the electrophoretic

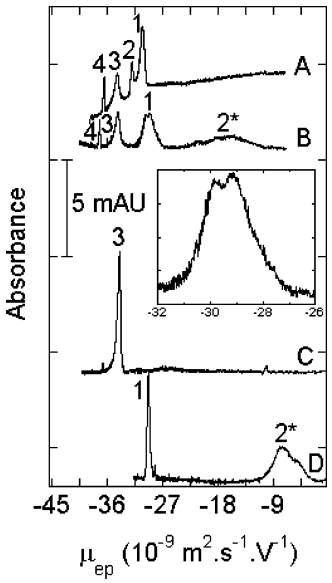


**Figure 4.** Influence of the addition of neutral surfactant micelles (Brij 35) in the electrolyte. 115−140 diblock copolymer purified by method 2 without Brij 35 (A) and with $C_{Brij35} = 5$ mM (B), homopolymer PAA ($DP_{PAA} = 115$) purified by method 3 with $C_{Brij35} = 0.5$ mM (C), and 75−20 copolymer purified by method 1 with $C_{Brij35} = 1$ mM (D). Identification: peak 2*, free copolymer in interaction with a Brij 35 micelle. Other conditions and identifications as in Figure 2.

mobility of the decorated nonionic surfactant micelles. It is worth noting that the equilibrium between the free copolymer and the Brij micelle was quickly reached since similar results were obtained by injecting the copolymer sample in the presence or absence of neutral surfactant.

For all the copolymers, the fraction of unimer−Brij micelle complexes (column B, Table 3) was higher than the fraction of unimers before the addition of Brij (column A, Table 2). Some of the copolymer micelles must have been destabilized by the Brij micelles. This destabilization of the copolymer micelles was stronger for short corona thickness and low aggregation number as exemplified by the 75−20 copolymer.

The electropherogram of 115−140 copolymer in the presence of Brij 35 shows a splitting of the micellar peak above around 1 mM of surfactant (see zoom of peak 1 of electropherogram B in Figure 4). It probably results from the coexistence of unperturbed copolymer micelles and copolymer micelles which have incorporated some nonionic surfactant molecules. The addition of neutral micelles in the electrolyte was a simple manner to better separate peaks 1 and 2 and was also a good assessment of the peak 2 assignment.

**4.3.1.2. Equilibrium Constant of Association between the Free Copolymer and the Neutral Surfactant Micelle**. The electrophoretic mobilities of the 115−140 copolymer micelles (peak 1), the unimers (peak 2*), and the PAA (peak 3) were plotted as a function of the nonionic surfactant concentration contained in the electrolyte (Figure 5). The electrophoretic mobilities of peaks 1 and 3 were nearly constant or slightly decreased for high Brij concentrations because of the slight raise in the electrolyte viscosity. We observe a steep decrease of the electrophoretic mobility of peak 2 (or 2*) for a Brij concentration corresponding to the critical aggregation concentration (cac) of the neutral surfactant. It clearly indicates that the copolymers interact with surfactant micelles. From Figure 5, the cac is between 0.04 and 0.085 mM. These values are close to cmc of Brij 35 in water (0.1 mM).[18] This observation is in good agreement with the previous explanation concerning the complex structure composed of a decorated surfactant micelle with one block copolymer chain.

Assuming that the unimers are in equilibrium between two states—free unimer in solution and associated unimer in interaction with one Brij micelle (decorated surfactant micelle)—the electrophoretic mobility of the copolymer $\mu_{ep}$ as a function of the Brij concentration $C_{Brij}$ is given by

$$\mu_{ep} = \frac{C}{C + C^*}\mu_{ep}^{\ 2} + \frac{C^*}{C + C^*}\mu_{ep}^{\ 2^*} \qquad (9)$$

where $C$ is the concentration of free unimer, $C^*$ is the concentration of the decorated surfactant micelle, $\mu_{ep}^{\ 2}$ is the electrophoretic mobility of the free copolymer (without Brij), and $\mu_{ep}^{\ 2*}$ is the electrophoretic mobility of the surfactant micelle decorated with one copolymer chain.

Equation 9 leads to the following relationship:

$$\mu_{ep} = \frac{1}{1 + K\dfrac{C_{Brij} - cac}{N}}\left[\mu_{ep}^{\ 2} + K\frac{C_{Brij} - cac}{N}\mu_{ep}^{\ 2*}\right] \qquad (10)$$

where $N$ is the aggregation number of the Brij micelle and $K$ the equilibrium constant. Equation 10 is valid only for $C_{Brij} >$ cac. With $\mu_{ep}^{\ 2} = -32.1 \times 10^{-9}$ m$^2$ s$^{-1}$ V$^{-1}$ and $\mu_{ep}^{\ 2*} = -16.0 \times 10^{-9}$ m$^2$ s$^{-1}$ V$^{-1}$, the curve fitting in Figure 5 led to $K/N = 16.0 \pm 0.2$ mM$^{-1}$ and cac $= 0.042 \pm 0.002$ mM. The cac value is slightly lower than the cmc of the Brij micelle in water. Taking a $N$ value similar to the aggregation number of an isolated surfactant micelle ($N = 40$ [21]), $K = 640 \pm 8$ mM$^{-1}$.

**4.3.1.3. Modelization of the Electrophoretic Mobility of the Decorated Brij Micelle.** To obtain better insight into the structure of the decorated surfactant micelle, the models described in section 2 about the electrophoretic mobility of composite objects were confronted to the experimental values (see Table 3). The composite object considered in this section is composed of a free copolymer diblock in interaction with only one Brij 35 (decorated micelle).

We first tried to apply the model used for the free diblock copolymer (eq 3). In this model, there is a strong hydrodynamic coupling between the PAA block and the Brij micelle, as depicted in Figure 1A, where the neutral block is fully wrapped by the polyelectrolyte chain. Note that $2R_{Brij}$ is higher than the Debye length, and thus, the diameter of the Brij micelle can be taken as the dimension of the equivalent blob (see section 2.2.1 for the description of this model). Since $R_{Brij} < l_p$, the PAA chain is stretched at the scale length of an equivalent blob. Thus, the number of charged monomers ($\alpha$) in one equivalent blob equals to $2R_{Brij}/a$, where $a$ is the acrylate monomer size ($a = 0.3$ nm). We also assume that the hydrodynamic radius of the decorated micelle was equal to the hydrodynamic radius of the surfactant micelle. The agreement of the theoretical values derived from eq 3 with the experimental data was not good, the calculated values being overestimated. The high dimension of the Brij micelle, combined with the stiffness of the PAA chain, could explain this mismatch since the PAA should not be able to envelop the Brij micelle.

**Table 3. Experimental and Theoretical Electrophoretic Mobilities of the Decorated Brij Micelle with a Unimer[a]**

| | | electrophoretic mobilities of peak 2* ($10^{-9}$ m$^2$ V$^{-1}$ s$^{-1}$) | | | |
|---|---|---|---|---|---|
| analytes | $B$ | $\mu_{ep}^2$* | $(\mu_{ep}^2*)_{eq\ 3}$ | $(\mu_{ep}^2*)_{eq\ 4}$ | $(\mu_{ep}^2*)_{eq\ 5}$ |
| 115−140$^{(2)}$ | 0.45 | −16.5 | −28.5 | −9.9 | −17.0 |
| 75−20$^{(1)}$ | 0.49 | −7.7 | −14.9 | −4.1 | −6.8 |
| 185−55$^{(2)}$ | 0.25 | −11.0 | −22.8 | −6.6 | −11.2 |

[a] The electrophoretic mobility of the polyelectrolyte taken in all equations is $\mu_{ep}^0 = -34.4 \times 10^{-9}$ m$^2$ V$^{-1}$ s$^{-1}$. The fraction of copolymer associated with a Brij micelle relative to the total copolymer concentration is given in column $B$.

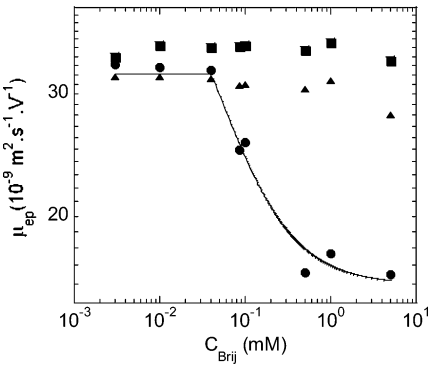


**Figure 5.** Variation of the electrophoretic mobilities in absolute value of the copolymer micelle (▲), the free copolymer (●), and the PAA (■) for the 115−140 copolymer solution as a function of the nonionic surfactant concentration. The line corresponds to the curve fitting of the electrophoretic mobility data (peak 2*) according to eq 10. Other conditions as in Figure 2.

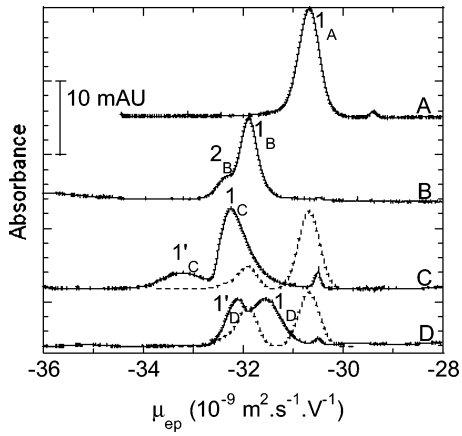


**Figure 6.** Elecropherograms of pure block copolymers 75−20 (A) and 185−55 (B). Binary mixtures of diblock copolymer micelles. 72/28 w/w mixture of 75−20 and 185−55 copolymers (C), 50/50 w/w mixture of 75−20/ 185−55 copolymers (D). 75−20 copolymer was purified according to method 1, and 185−55 copolymer was purified according to method 3. Other conditions as in Figure 2. Sums of electropherograms A and B weighted by the corresponding proportion in the mixture (· · ·). Peaks designation after mixing: $1_C$ and $1'_C$ for electropherogram C and $1_D$ and $1'_D$ for electropherogram D.

Equation 4 should thus be more suitable since it is based on (i) a segregation between the two moieties of the decorated micelle and (ii) on a coil conformation of the PAA block. The agreement between experimental calculated values was much better than using eq 3 (see Table 3); however it was not perfect, especially for the copolymer with the smallest PAA blocks (75−20 and 185−55). For these latter copolymers, the contour lengths of their PAA blocks were below or in the same order of one Kuhn length (equal to twice the persistence length, i.e., 34 monomers). Therefore, PAA blocks were too short to allow a true coil conformation. The third model (eq 5), assuming that the PAA chain is fully stretched, was more appropriate (see Table 3).

The good agreement between the values derived from eq 5 and the experimental data seems to corroborate that the hydrophobic block of the copolymers interacted with only one Brij micelle. It is worth noting that, up to our knowledge, we report here the first experimental observation of the existence of the regime described by eq 5.

**4.3.2. Mixed Micelles of Two Copolymers.** In this section, experiments based on the mixing of two different populations of diblock copolymer micelles (75−20 precipitated in water and 185−55 purified by dialysis) having different electrophoretic mobilities were performed. The electropherograms C and D obtained for two different mixtures of micelles in different proportions are presented in Figure 6. For comparison, electropherograms of pure 75−20 and pure 185−55 copolymers are also presented (electropherograms A and B). Dotted lines in electropherograms C and D correspond to the sums of electropherograms A and B weighted by the corresponding proportion in the mixture.

In both mixtures, the experimental electropherograms show two main peaks. Their relative time corrected area follows the composition of the mixture with a slight enrichment of peak 1. The fraction of peak 1 is 0.59 for the 50/50 w/w mixture of 75−20/ 185−55 and 0.8 for the 72/28 w/w copolymers mixture. This observation suggests that exchange of matter concerns only a small amount of copolymers or that the exchange coincidentally leads to two micelles populations in the same proportions. By increasing temperature of the 50/50 mixture from 30 up to 40 °C, the fraction of peak 1 increases further up to 0.65. This value remains constant between 40 and 50 °C. The corresponding fraction of the enrichment of peak 1 is of the same order as the fraction of 185−55 isolated micelles destabilized by an increase in temperature (see section 4.2.5).

Surprisingly, the electrophoretic mobilities of both micelles in the mixture are quite different from the electrophoretic mobilities of the initial micelles. Moreover, they depend on the composition of the binary mixture.

Finally, from these results, it seems that the two populations of micelles do not completely mix to lead to a single micelle population. However, reorganization between the two micelle populations should not be excluded as the electrophoretic mobilities of the micelles do not remain constant after mixing.

## 5. Conclusion

Despite the inherent limitations of on-line UV detection for structure elucidation, most of the peaks detected during the electrophoretic separation of PVAc-*b*-NaPAA copolymer solutions were identified on the basis of electrophoretic mobility values, relative abundances, sample spiking, and electrophoretic behavior in the presence of surfactant micelles. CE provided further

insight into the distribution between free and self-assembled forms of the copolymers. A significant amount of free copolymers was separated from the micelles. This free unimer population is not in exchange with the micelle because these free copolymers are unable to self-assemble due to their chemical composition. Those free copolymers could either be composed of a shorter hydrophobic block and/or a longer hydrophilic block than the copolymer constituting the micelle or could be more hydrolyzed. The repartition of the copolymer between the micelles and the free form has been clearly shown to depend on the purification procedure of the diblock and also on its molecular architecture. Above a critical temperature, of the order of the glass transition temperature of the hydrophobic block, the fraction of free copolymer significantly increases. On the other hand, the diblock concentration has no effect on the relative amount of free and self-assembled copolymers. Capillary electrophoresis allows controlling the quality of the diblock synthesis and purification by detecting the eventual presence of poly(acrylic acid) and acetate at the end of the synthesis process.

The modeling of the electrophoretic mobility of the copolymer micelles as a function of the copolymer chemical composition remains a challenging issue that requires further experimental work and the use of other theoretical developments than those used in this work. Nevertheless, the recent theoretical developments[16] concerning the electrophoretic mobility of composite objects have already shown that they are very useful to better understand the electrophoretic behavior of block copolymer and to help in the identification of the peaks.

A recent methodology described by Berezovski et al.[22] for the study of DNA proteins, named nonequilibrium CE of equilibrium mixtures, has the potential to reveal binding and kinetic rate constants of the unimer/micelle equilibrium. While the presence of the stationary phase ruins this possibility in SEC, the analysis of the micelle peak profile in CE should give quantitative information on the aforementioned equilibrium, as far as the kinetics of exchange would be fast enough at the time scale of the CE experiment.

## References and Notes

(1) Hajduk, D. A.; Kossuth, M. B.; Hillmyer, M. A.; Bates, F. S. *J. Phys. Chem. B* **1998**, *102*, 4269.
(2) Munk, P. In *Solvents and Self-Organization of Polymers*; Weber, S. E., et al., Eds.; Kluwer Academic Publishers: Dordrecht, The Netherlands, 1996; pp 367−381.
(3) Pedersen, J. S. *Adv. Colloid Interface Sci*. **1997**, *70*, 171.
(4) Xu, R.; Hu, Y.; Winnik, M. A.; Riess, G.; Croucher, M. D. *J. Chromatogr.* **1991**, *547*, 434.
(5) Cottet, H.; Gareil, P.; Guenoun, P.; Muller; Delsanti, M.; Lixon, P.; Mays, J. W.; Yang, B.-S. *J. Chromatogr. A* **2001**, *939*, 109.
(6) Gaillard, N.; Guyot, A.; Claverie, J. *J. Polym. Sci., Part A: Polym. Chem.* **2003**, *41*, 684.
(7) Khougaz, K.; Gao, Z.; Eisenberg, A. *Macromolecules* **1994**, *27*, 6341.
(8) Morishima, Y. *J. Polym. Sci.* **2000**, *18*, 323.
(9) Stepanek, M.; Podhajecka, K.; Tesarova, E.; Prochazka, K. *Langmuir* **2001**, *17*, 4240.
(10) Corpart, P.; Charmot, D.; Biadatti, T.; Zard, S. Z.; Michelet, D. WO 9858974, Rhodia Chimie, 1998.
(11) Charmot, D.; Corpart, P.; Adam, H.; Zard, S. Z.; Biadatti, T.; Bouhadir, G. *Macromol. Symp.* **2000**, *150*, 23.
(12) Khaledi, M. G. In *High Performance Capillary Electrophoresis: Theory, Techniques and Applications*; Khaledi, M. G., Ed.; John Wiley and Sons: New York, 1998.
(13) Anderson, J. L.; Solomentsev, Y. *ACS Symp. Ser.* **1994**, 67.
(14) Long, D.; Ajdari, A. *Electrophoresis* **1996**, *17*, 1161−1166.
(15) Long, D.; Viovy, J. L.; Ajdari, A. *J. Phys.: Condens. Matter* **1996**, *8*, 9471.
(16) Desruisseaux, C.; Long, D.; Drouin, G.; Slater, G. W. *Macromolecules* **2001**, *34*, 44.
(17) Tricot, M. *Macromolecules* **1984**, *17*, 1698.
(18) Collet, J.; Tribet, C.; Gareil, P. *Electrophoresis* **1996**, *17*, 1202.
(19) Morel, A. Ph.D. Thesis, University of Montpellier 2, France, 2004.
(20) Brandup, J.; Immergut, E. H. *Polymer Handbook*; John Wiley & Sons: New York, 1989.
(21) Nishi, H.; Terabe, S. *J. Chromatogr. A* **1996**, *735*, 3.
(22) Berezovski, M.; Krylov, S. N. *J. Am. Chem. Soc.* **2002**, *124*, 13674.

MA050586F